



## Antiradical and Anti-inflammatory Activity of *Saccharomyces cerevisiae*-Mediated Selenium Nanoparticles

Aya Adel Fath-Alla<sup>1</sup>, Neveen M. Khalil<sup>1</sup>, Ayman Saber Mohamed<sup>2</sup> and Mohamed N. Abd El-Ghany<sup>1\*</sup>



<sup>1</sup> Botany and Microbiology Department, Faculty of Science, Cairo University, Giza 12613, Egypt

<sup>2</sup> Zoology Department, Faculty of Science, Cairo University, Giza 12613, Egypt

**T**HE PRESENT research study aimed for the biosynthesis of selenium nanoparticles (SeNPs) using *Saccharomyces cerevisiae* (baker's yeast) as a sustainable, green, eco-friendly, and economically suitable source. The yeast-mediated SeNPs were characterized to detect their physicochemical properties by using UV-Vis, TEM, DLS, FTIR, and XRD analyses. The biosynthesized SeNPs were spherical in shape with sizes ranging from 34 to 125 nm, carrying a negative charge that equals -22.4 mV, and had an amorphous nature. FTIR indicated that SeNPs were surrounded with bioactive proteins as reducing and capping agents produced by yeast cells. Various biological capacities of biosynthesized SeNPs were measured including cytotoxic, antiradical, anti-inflammatory, and antimicrobial activities. The cytotoxicity results showed that the yeast-mediated SeNPs are nontoxic particles with IC<sub>50</sub> value above 300 µg/mL. Therefore, they can be applied as a safe and green therapeutic agent. An antiradical assay revealed that SeNPs had the scavenging ability of DPPH. In addition, anti-inflammatory tests ensured the capacity of SeNPs to inhibit nitric oxide released from macrophage cells due to induced inflammation. Both antiradical and anti-inflammatory actions were shown at noncytotoxic SeNP concentrations. The highest antiradical activity (63.26%) was shown at 150 µg/mL SeNPs, and the highest anti-inflammatory action (41.34%) was observed at 100 µg/mL SeNPs. Subsequently, yeast-derived SeNPs are a safe, alternative, and sustainable agent that can be used as an antiradical and anti-inflammatory drug at their noncytotoxic levels (1-300 µg/mL).

**Keywords:** *Saccharomyces cerevisiae*, Selenium nanoparticles, Cytotoxicity, Antiradical properties, Anti-inflammatory properties, Anti-microbial properties.

### Introduction

Nanotechnology deals with materials at the nanoscale (1 to 100 nm). Nanoparticles (NPs) have a larger surface-area-to-volume ratio, increased chemical reactivity, and high stability (Hussain et al., 2010; Dubadi et al., 2023). These characteristics give NPs unique physical, chemical, and biological properties that enhance their use in various applications (Nowack and Bucheli, 2007; Abd El-Ghany et al., 2023). Nanoparticles are incorporated in various fields such as agricultural, biomedical, environmental, and industrial fields (Khan et al., 2019).

Inorganic nanoparticles can be synthesized by physical, chemical, and biological methods. Physical approaches are achieved by applying forces such as degradation, cutting, and grinding; however, these processes are expensive, need high energy, consume time, and form NPs with large sizes and defective surfaces (Mudshinge et al., 2011; Saratale et al., 2018). Chemical methods use toxic chemicals that cause environmental pollution

and limit their biomedical application (Abegunde et al., 2019). Biological methods are considered green, ecofriendly, nontoxic, low-cost, and rapidly developing methods (Alsammarrarie et al., 2018; Devi et al., 2019; Ying et al., 2022). These methods use plants, algae, fungi, yeast, and bacteria as reducing, capping, and stabilizing agents (Mudshinge et al., 2011; Arokiyaraj et al., 2015; Saratale et al., 2018). Biosynthesized NPs may be used in the medical field as they are nontoxic, biocompatible, and biodegradable (Li et al., 2011; Khalil et al., 2019). Nanoparticles can act as antimicrobial, antiradical, anticancer, anti-inflammatory, antidiabetic, and drug-delivery agents (McNamara and Tofail, 2017)

Microorganisms are widely used in the biosynthesis process because they grow rapidly, need simple requirements, and produce NPs via intracellular or extracellular ways (Li et al., 2011; Carrapiço et al., 2023). Fungi as a biological source of NP production can be handled easily and cultured on a large scale producing large amounts of biomass and various enzymes which provide high NP yield

\*Corresponding author emails: dr.mohamed.naguib@cu.edu.eg - Mabelghany@sci.cu.edu.eg

Received: 02/02/2024; Accepted: 29/04/2024

DOI: 10.21608/ejbo.2024.267306.2692

Edited by: Prof. Dr. Khaled Ghanem, Microbiology-Bacteriology, Faculty of Science, Alexandria University, Egypt

©2024 National Information and Documentation Center (NIDOC)

(Hulkoti and Taranath, 2014). Biosynthesis of metal NPs using yeast is preferred as compared to those which use other types of microorganisms due to the easy control of yeast biomass production and fast growth using simple nutrient culture media (Sasidharan and Balakrishnaraja, 2014; Faramarzi et al., 2020). Different yeast strains depend on various mechanisms to synthesize various-sized and monodispersed NPs (Hulkoti and Taranath, 2014).

*Saccharomyces cerevisiae* is one of the promising yeast species that have been used in the production of different nanoparticles having many biological activities. Silver nanoparticles synthesized by *Saccharomyces cerevisiae* can be used as an antimicrobial agent against *Staphylococcus aureus*, *Escherichia coli* (Korbekandi et al., 2016; Kharchenko et al., 2022), and *Klebsiella pneumoniae* (Kharchenko et al., 2022). *Saccharomyces cerevisiae*-synthesized zinc oxide nanoparticles have antimicrobial (Motazed et al., 2020; El-Khawaga et al., 2023), antioxidant, and anticancer potential (Motazed et al., 2020). Gold nanoparticles synthesized by using Baker's yeast (*Saccharomyces cerevisiae*) exhibit anticancer action against Ehrlich ascites carcinoma cells (Attia et al., 2016).

Selenium (Se) is an essential trace element that is incorporated as selenocysteine in various antiradical enzymes like glutathione peroxidase and selenoprotein P (Khurana et al., 2019). The selenium element has a narrow therapeutic application while the presence of selenium in nanoform provides additional properties. SeNPs possess wide therapeutic benefits and are used as antimicrobial, antiradical, anti-inflammatory (Khurana et al., 2019; Pandiyan et al., 2022), antiulcerative (Bai et al., 2020), anticancer (Martinez-Esquivias et al., 2022), and drug-delivery agents (Khurana et al., 2019). Low toxicity and biocompatibility of biofabricated SeNPs enable them to be used as a safe drug. A comparative study done by Forootanfar et al. (2014) detected that the biosynthesized SeNPs have lower toxicity than  $\text{SeO}_2$ . SeNPs are a promising drug because of their low toxicity and high bioavailability. Also, the very small particle size of SeNPs increases their absorption through human and animal gastrointestinal tracts (Xu et al., 2019; Karthik et al., 2024). It was found that yeast-synthesized SeNPs had maximum antiradical activity. The obtained results can be related to the small particle size of the synthesized SeNPs (Faramarzi et al., 2020). SeNPs have anti-inflammatory activity (Francis et al., 2020) and can reduce the level of tumor necrosis factor-alpha (TNF- $\alpha$ ) (Miroliaee et al., 2011). Biogenic SeNPs synthesized by *Lactococcus lactis* NZ9000 showed powerful activity to regulate and reduce inflammation effect (Xu et al., 2019). SeNPs synthesized by

*Saccharomyces cerevisiae* showed a promising antimicrobial action against some bacterial and fungal species such as *Staphylococcus aureus*, *Escherichia coli*, *Aspergillus fumigatus*, and *Aspergillus niger* (Salem, 2022).

*Saccharomyces cerevisiae* is considered as a promising microorganism in the biofabrication of NPs because it has all the properties of fungi besides a nontoxic value since it is an edible fungus. The present study aimed to (1) biofabricate SeNPs by using *Saccharomyces cerevisiae*, (2) characterize the formed SeNPs by various methods, (3) evaluate SeNPs toxicity, and (4) detect the biomedical activities of SeNPs including antiradical, anti-inflammatory, and antimicrobial activities. This research is expected to provide the biomedical field with a newly eco-friendly, green, and less toxic drug to be used in different medical aspects.

## Materials and Methods

### 1. Biosynthesis of Selenium Nanoparticles

Industrial *Saccharomyces cerevisiae* yeast powder was purchased from Angel Company. One gram of *Saccharomyces cerevisiae* powder inoculated in 100 mL sterile Sabouraud dextrose broth (SDB) and then 0.025 g of sodium selenite ( $\text{Na}_2\text{SeO}_3$ ) was added (Faramarzi et al., 2020). The culture was incubated at dark conditions in a static incubator at 30°C for 24 h. Under the same conditions, a control was prepared containing SDB medium and  $\text{Na}_2\text{SeO}_3$  salt without yeast cells. After incubation time, the color of the tested culture media changed into red indicating the intracellular synthesis of SeNPs by yeast. *S. cerevisiae* cells were separated from the mixture by centrifugation at 5000 rpm for 5 min. SeNPs were obtained from the cells through cell destruction by sonication at 40 kHz for 30 min. Then SeNPs were separated from the remains of yeast cells by using a cooling centrifuge at 10000 rpm for 10 min at 4°C and washing with deionized water several times. The pure SeNPs were dried by a lyophilization technique, sterilized by wet heat sterilization technique using an autoclave for 20 min at 121°C and 1.5 bar in order to eliminate any microbial contaminants (Sasidharan and Balakrishnaraja, 2014; Visha et al., 2015), and stored at 4°C for further analysis (Faramarzi et al., 2020).

### 2. Characterization of Selenium Nanoparticles

SeNPs were characterized to identify their physicochemical properties by several methods. The formation of SeNPs was detected by using UV-Vis spectrophotometer (model Perkin-Elmer Hitachi 2000) (Botany and Microbiology Department, Faculty of Science, Cairo University) where the absorbance was measured at a range of wavelengths of 330 to 410 nm. The distribution and

morphology including shape and size of SeNPs were obtained by transmission electron microscopy (TEM, a Jeol JEM-1400) (Cairo University Research Park, Faculty of Agriculture). A droplet of SeNPs dispersed in acetone was placed on a copper grid and the excess of acetone was evaporated at room temperature. The dynamic light scattering (DLS) analyzer (PSS-NICOMP, Santa Barbara, CA, USA) at the Egyptian Petroleum Research Institute, Cairo, Egypt, was used to measure particle size, size distribution, and zeta potential at room temperature. The dried powder of SeNPs was suspended in deionized water to be prepared for these measurements. The spectrum of the dried sample of SeNPs was determined at a wavelength range of 400–4000  $\text{cm}^{-1}$  using the Fourier-transform infrared (FTIR, 6100) spectrophotometer at the Microanalytical Center, Faculty of Science, Cairo University. X-ray diffraction technique was used to detect X-ray diffraction patterns and study the crystalline structure of SeNPs using X-ray diffractometer (6000, Shimadzu, Japan) at the Microanalytical Center, Faculty of Science, Cairo university in the range of  $2\theta = 10\text{--}70^\circ$  (Anandalakshmi et al., 2016)

### 3. In Vitro Biological Application

#### 1) Antimicrobial Activity

Antimicrobial activity of the biosynthesized SeNPs was assessed by using agar well diffusion method. SeNPs were tested against various types of microorganisms including bacteria and fungi. *Staphylococcus aureus* MRSA (ATCC 43300) and *Bacillus cereus* (ATCC 33018) were used as Gram-positive and *E-coli* O:157 (ATCC 93111) and *Pseudomonas aeruginosa* (ATCC 9027) as Gram-negative bacterial strains. Under aseptic conditions, half MacFarland ( $1.5 \times 10^5$  CFU/mL and turbidity with OD = 0.13 at 625 nm) of each tested bacterial strain was inoculated on sterile triplicate plates of Mueller-Hinton agar by the spreading technique. Sterile 100  $\mu\text{L}$  of SeNP suspension at a concentration of 1000  $\mu\text{g}/\text{mL}$  was added to each agar well that was cut out by using sterile cork borer, 3 wells/plate. After that, all Petri plates were incubated at 37°C for 24 h. By the same procedures with a slight difference, SeNPs were tested against *Candida albicans* (ATCC 10231) as a selected fungal strain. One mL fungal spore suspension ( $10^7$  spores/mL) was inoculated on triplicate plates of potato dextrose agar (PDA) and incubated at 30°C for 2-4 days. After incubation time, the diameter of the inhibition zone was measured and expressed as mm (Hashem et al., 2021).

#### 2) Cytotoxicity Assay

##### a) Preparation of a Normal Cell Line

The tested mouse normal liver cells (BNL) were acquired from Nawah Scientific Inc. (Mokatam-

Cairo, Egypt). Cells were maintained in Dulbecco's Modified Eagle Media (DMEM) supplemented with streptomycin (100 mg/mL), penicillin (100 units/mL), and heat-inactivated fetal bovine serum (10%) in a humidified atmosphere containing 5% (v/v)  $\text{CO}_2$  at 37°C. DMEM is a basal medium used to support cell growth (Skehan et al., 1990).

##### b) Preparation of a Selenium Nanoparticle Suspension

Sterile powder of SeNPs was suspended in cell culture media to prepare nine different concentrations (1, 3, 10, 30, 100, 150, 200, 250, and 300  $\mu\text{g}/\text{mL}$ ).

##### c) The Sulforhodamine B (SRB) Cytotoxicity Assay

In each well of 96-well microtiter plates, 100  $\mu\text{L}$  cell suspension containing  $5 \times 10^3$  cells was seeded in complete growth media for 24 h. Then, cells were treated with 100  $\mu\text{L}$  media containing SeNPs at different concentrations (1, 3, 10, 30, 100, 150, 200, 250, and 300  $\mu\text{g}/\text{mL}$ ) for 72 h. After drug exposure time, cells were fixed by using 150  $\mu\text{L}$  of 10% trichloroacetic acid (TCA) and incubated at 4°C for 1 h. Then, a TCA solution was removed and the cells were washed 5 times with distilled water. The cells in each well were stained by adding 70  $\mu\text{L}$  sulforhodamine B (SRB) solution (0.4% w/v) that attaches to the basic amino acids of cellular proteins. The plate was incubated in dark condition at room temperature for 10 min, washed 3 times with 1% acetic acid to remove excess stain, and then allowed to dry in air overnight. SRB bound to cellular proteins was dissolved by adding 150  $\mu\text{L}$  TRIS (10 mM). The absorbance of the free SRB stain was measured at 540 nm by using a BMG LABTECH's FLUOstar Omega microplate reader (Ortenberg, Germany) (Skehan et al., 1990). The percentage of cell viability was calculated based on the following equation. Control cells represent incubated cells without SeNPs.

Percentage of cell viability (%) = (absorbance of control cells - absorbance of tested sample) x 100/ absorbance of control cells.

The  $\text{IC}_{50}$  was also calculated. It is the concentration that inhibits 50 % of viable cells.

#### 3) Antiradical Activity Using DPPH Assay

Free radical scavenging activity of the biogenic SeNPs was estimated using 1,1-diphenyl-2-picrylhydrazyl (DPPH) assay according to the method used by Ansari et al. (2013). Five different concentrations of SeNPs dissolved in methanol were prepared (50, 100, 150, 200, and 250  $\mu\text{g}/\text{mL}$ ). DPPH solution was prepared by dissolving 0.078 g DPPH in 100 mL of methanol. One milliliter of each SeNP concentration was mixed with 1 mL of the prepared DPPH and incubated at 37°C for 30

min in dark conditions. Two mL prepared DPPH was used as a control and incubated at the same conditions. Ascorbic acid was used as standard. After the incubation time, the absorbance of the reaction mixture was measured at 517 nm by utilizing a UV-Vis spectrophotometer. The percentage of free radical scavenging activity was calculated according to the following equation:

$$\text{DPPH free radical scavenging activity (\%)} = \frac{(\text{absorbance of control cells} - \text{absorbance of sample}) \times 100}{\text{absorbance of control cells}}$$

The IC<sub>50</sub> was also calculated. It is the inhibitory concentration that is required for scavenging 50% of free radicals.

#### 4) Anti-Inflammatory Activity

##### a) Preparation of a Normal Cell Line

A mouse macrophage cell line (RAW264.7 cells) was the used tested cell line for anti-inflammatory assay and it was acquired and prepared as BNL cells, as abovementioned.

##### b) Cytotoxicity of SeNPs on RAW264.7 Cells

Five concentrations (20, 30, 40, 50, and 100 µg/mL) of SeNPs were used to assess the cytotoxic effect on RAW264.7 cells using the SRB assay as abovementioned in the case of BNL cells.

##### c) Measurement of Nitric Oxide

RAW264.7 macrophage cells were seeded into a 96-well microtiter plate and incubated for 24 h. After the incubation period, cells were classified into three groups: treated, LPS, and blank groups. The treated group is the cells that were treated with 5 concentrations of the tested SeNPs (20, 30, 40, 50, and 100 µg/mL) for 2 h. Then, 1 µg/mL of lipopolysaccharide (LPS) was added for 48 h to induce inflammation and nitric oxide (NO) production. The LPS group is the cells that were stimulated with LPS while the blank group is the cells that were replenished with fresh media. The amount of released NO was measured by using Griess reagent. Equal volumes of both supernatant and Griess reagent were mixed in a dark condition at room temperature for 10 min. Nitric oxide concentration was detected by measuring the absorbance of mixture at 540 nm using an ELISA plate reader (aBMGLABTECH's FLUOstar Omega microplate reader (Ortenberg, Germany), and the percentage of inhibition was calculated based on the following equation (Kim et al., 2021; Ahmed et al., 2022):

$$\text{Inhibition (\%)} = \frac{(\text{absorbance of control cells} - \text{absorbance of sample}) \times 100}{\text{absorbance of control}}$$

#### 4. Statistical Analysis

The data presented in each experiment were the mean of values of three experiments ± SE with

significantly different  $p < 0.05$ . The SPSS 20.0 software was used for the determination of mean, standard error, and least significant difference (LSD) of values.

## Results and Discussion

### 1) Biosynthesis of SeNPs

After the incubation period (24 hrs), the color of *Saccharomyces cerevisiae* culture containing sodium selenite (tested sample) changed into red color which refers to the reduction of sodium selenite (Se<sup>IV</sup>) to selenium element (Se<sup>0</sup>) in the nanoparticle form, while there was no change in the control (Figure 1a). This indicates that yeast is totally responsible for the biosynthesis of SeNPs. *Saccharomyces cerevisiae* produce proteins and enzymes (reductase) for the biosynthesis process including bioreduction, stabilization, and capping process (Bartosiak et al., 2019).

### 2) Characterization

#### 2.1. UV-Visible Spectroscopy

Formation of SeNPs was confirmed by measuring the absorption of red color at various wavelengths using UV-visible spectrophotometer. The red color of SeNPs was due to the excitation of their surface plasmon resonance (SPR) (Salem, 2022). SPR is a phenomenon that occurs when electrons in a thin metal sheet become excited by light. UV-Vis spectroscopic analysis indicated that the  $\lambda_{\text{max}}$  of SeNP solution appeared at 360 nm (Figure 1a). According to several studies,  $\lambda_{\text{max}}$  of SeNPs was detected at a range of wavelengths (250-350 nm) (Fardsadegh et al., 2019; Fardsadegh and Jafarizadeh-Malmiri, 2019; Faramarzi et al., 2020).

#### 2.2. Fourier Transform-Infrared Spectroscopy

FTIR is used to detect the presence of various functional groups of bioactive molecules present on the surface of SeNPs such as proteins, lipids, and carbohydrates. These biomolecules, especially proteins, are produced by *Saccharomyces cerevisiae* and act as reducing, stabilizing, and capping agents in the biosynthesis process (Bartosiak et al., 2019). As shown in Figure 1b the peaks in FTIR spectrum indicate the absorption of several vibrations corresponding to specific functional groups. X-axis represents wavenumber (cm<sup>-1</sup>) and Y-axis represents transmittance (%). Absorbances were represented by wavenumbers at 3428.81, 2921.63, 2853.17, 1642.09, 1454.06, 1246.75, 1045.23, 576.612, and 462.832 cm<sup>-1</sup>. The absorption band at 3428.81 cm<sup>-1</sup> was assigned to the stretching vibration of O-H and N-H, indicating the presence of alcohol (Jia et al., 2022) and amines of peptide chains and protein (Jalalian et al., 2018), respectively. Stretching vibration of C-H appeared at 2921.63 and 2853.17 cm<sup>-1</sup> due to the presence of aliphatic chains (-CH<sub>2</sub>- and -CH<sub>3</sub>)

present in lipids and protein side chains (Jia et al., 2022). The peak at  $1642.09\text{ cm}^{-1}$  is related to C=O stretching of the amide bond (–CO–NH) of peptide bonds of protein (Wu et al., 2021). The spectrum at  $1454.06\text{ cm}^{-1}$  is associated with carboxyl vibration (–COOH) (Tugarova et al., 2018; Lian et al., 2019). Absorption results at  $1246.75\text{ cm}^{-1}$  and  $1045.23\text{ cm}^{-1}$  are generated by C–O stretching of the carboxyl

group (Wu et al., 2021) and ether (Kora, 2018a), respectively. Table 1 summarizes the wavenumbers, bonds, and their corresponding functional groups. FTIR spectrum analysis interprets the presence of amines, amides, and carboxyl groups which represent protein molecules that may be the dominant bioactive compound surrounding SeNPs.

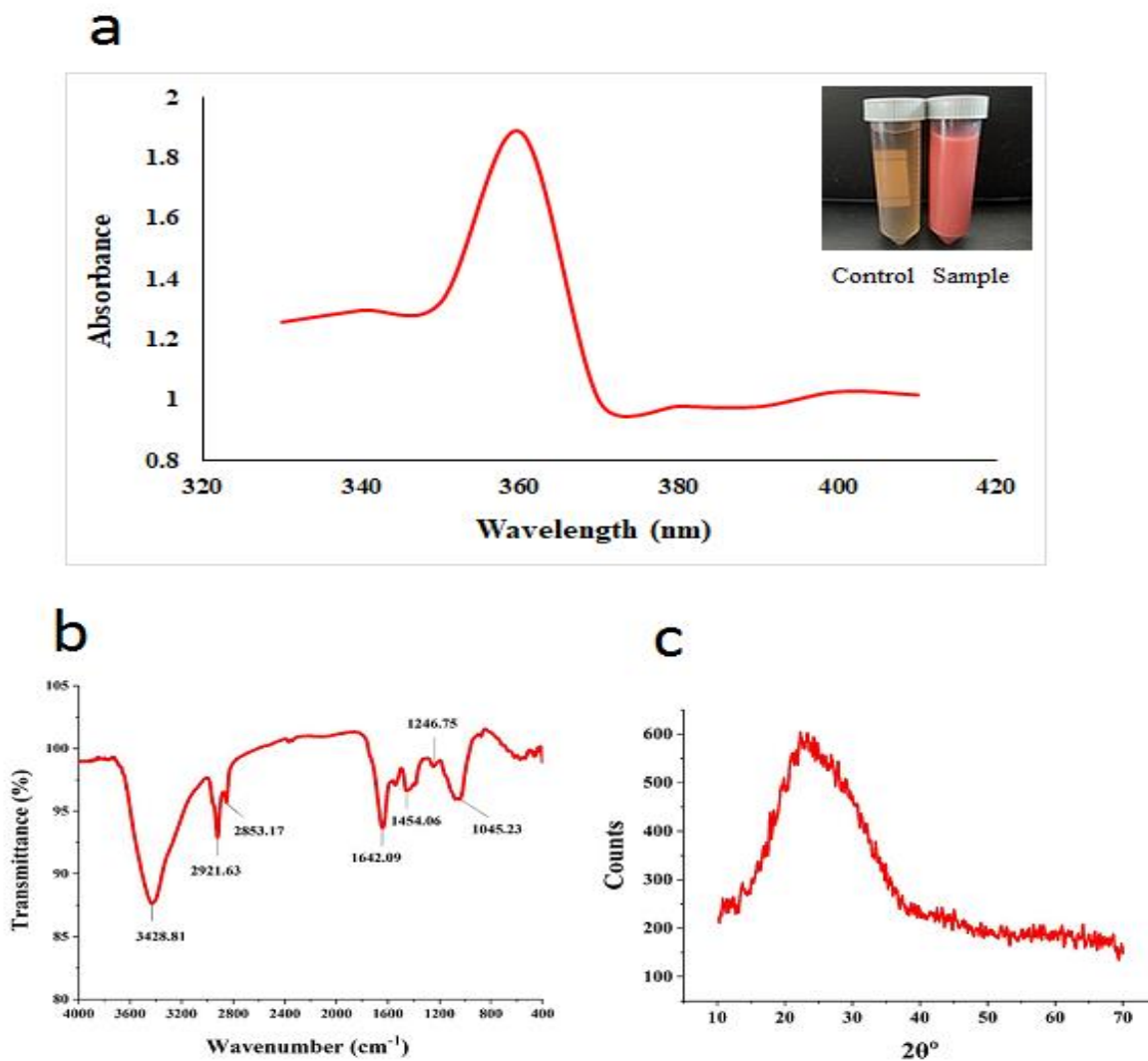


Fig. 1. (a) UV–Visible spectrum, (b) FTIR spectrum, and (c) XRD pattern of *Saccharomyces cerevisiae*-mediated SeNPs.

Table 1. Wavenumbers, bonds, and functional group of molecules surrounding yeast-mediated SeNPs

Wavenumbers ( $\text{cm}^{-1}$ )	Bonds	Functional groups	References
3428.81	O–H and N–H	Hydroxyl and amino	Jia et al., 2022; Jalalian et al., 2018)
2921.63 and 2853.17	C–H	Aliphatic chain	(Jia et al., 2022)
1642.09	C=O	Amide	(Wu et al., 2021)
1454.06	–COOH	Carboxyl group	(Tugarova et al., 2018; Lian et al., 2019)
1246.75	C–O	Carboxyl group	(Wu et al., 2021)
1045.23	C–O	Ether	(Kora, 2018a)

### 2.3. X-Ray Diffraction

The obtained pattern (Figure 1c) from X-ray diffraction analysis showed the broad peak at  $2\theta$  angles between  $23^\circ - 26^\circ$  which suggests that the synthesized SeNPs have an amorphous nature as also reported in several studies. As observed in the XRD pattern, the broadband at a low  $\theta$  degree indicates the amorphous nature, and sharp and strong bands refer to crystalline structure (Akçay and Avcı, 2020; Wu et al., 2021). These findings agree with the XRD pattern of biogenic SeNPs synthesized by yeast (Wu et al., 2021) and those synthesized by *Bacillus* sp. (Akçay and Avcı, 2020). In this regard, The XRD of mycosynthesized SeNPs using filtrate of *Alternaria alternata* culture provides that the formed NPs have an amorphous nature with a broad peak (Sarkar et al., 2011).

### 2.4. TEM and DLS Analysis

Both TEM and DLS are used to analyze the size of the biosynthesized SeNPs. According to TEM image in Figure 2a, the size of the yeast-mediated SeNPs ranged from 34 to 125 nm with spherical shape, while the obtained data from DLS analysis

detected that the average size was 173.9 nm as in Figure 2b. As DLS measures the hydrodynamic volume while TEM detects the core size of SeNPs. So, the average size of SeNPs measured through the DLS is higher than that measured by TEM (Huang et al., 2007; Srivastava and Mukhopadhyay, 2013; Wu et al., 2021; Salem, 2022). Other studies recorded the size of intracellular synthesized SeNPs from 75 to 709 nm using a range of sodium selenite salt (5 to 25  $\mu\text{g}$ ) (Faramarzi et al., 2020), while that of extracellular synthesized SeNPs was 83.3 nm (Salem, 2022). A polydispersity index (PDI) value of 0.503 indicates that the sample contains polydispersed SeNPs and there is a high stability of SeNPs in solution. Zeta potential value of these biogenic SeNPs was -22.4 mV (Figure 2c). It is an essential parameter that determines the surface charge of the nanoparticles and affects their stability. As the negative charge increases, the repulsion between SeNPs increases and aggregation of particles decreases causing high particle stability (Dang et al., 2014; Wu et al., 2021).

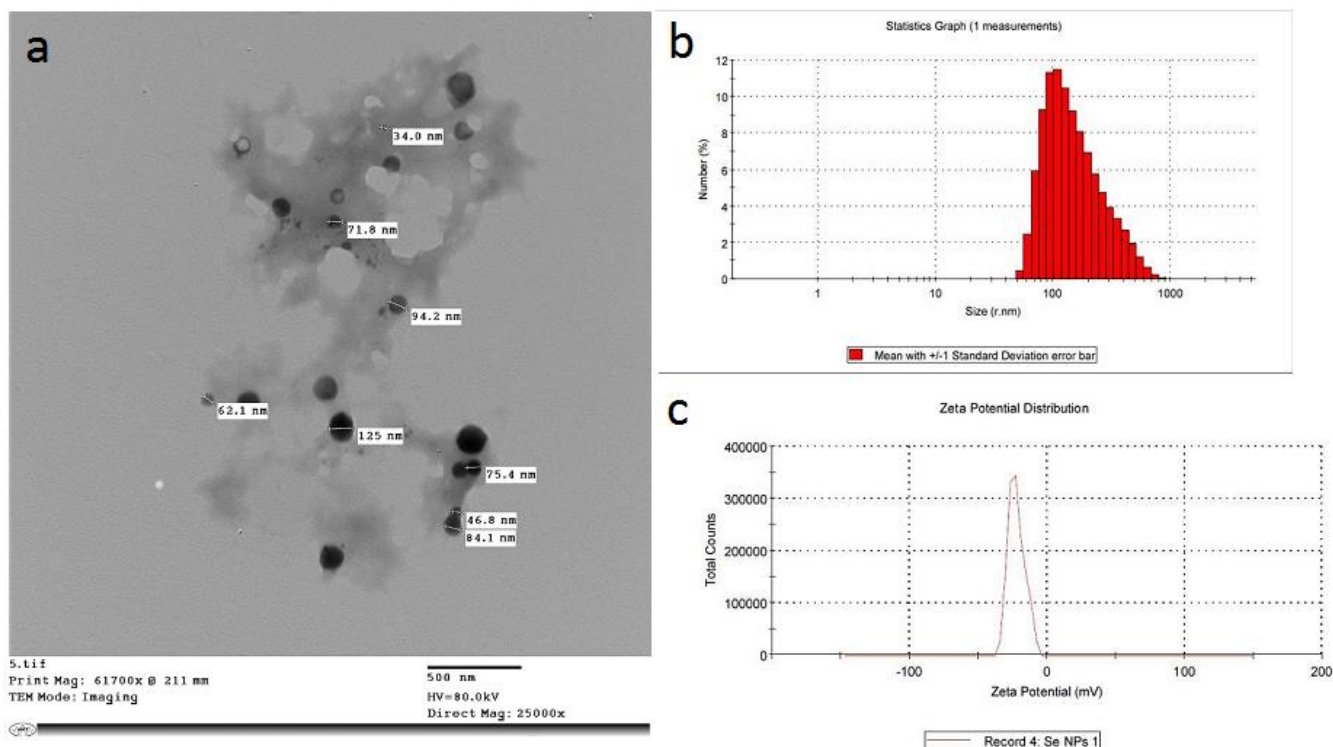


**Fig. 2. (a) TEM image, (b) DLS histogram, and (c) Zeta potential curve of intracellular synthesized SeNPs by *Saccharomyces cerevisiae*.**

### 3) Biological Applications

#### 3.1 Antimicrobial Activity

SeNPs at 1000  $\mu\text{g}/\text{mL}$  concentration were tested against Gram-positive bacteria (*Staphylococcus aureus* MRSA (ATCC 43300) and *Bacillus cereus* (ATCC 33018)), Gram-negative bacteria (*E-coli*

O:157 (ATCC 93111) and *Pseudomonas aeruginosa* (ATCC 9027)) and fungus (*Candida albicans* (ATCC 10231)).

After the incubation period, the formation of a clear zone around wells containing SeNPs was observed to detect the antimicrobial action of tested particles.

There were no inhibition zones formed indicating that the test SeNPs (100  $\mu\text{L}$ /well of 1000  $\mu\text{g}/\text{mL}$  concentration) have no antimicrobial action against the selected strains of bacterial and fungal species.

As also recorded by other studies, no inhibition zones were observed, when *Citricoccus* biosynthesized SeNPs were tested against Gram-positive *Staphylococcus aureus* (ATCC 23213) and Gram-negative *Escherichia coli* (ATCC 25922) (Dinc et al., 2022). Antibacterial test of tree gum stabilized SeNPs against Gram-negative bacteria showed no inhibition zone in both *Escherichia coli* 25922 and *Pseudomonas aeruginosa* 27853 (Kora, 2018b). SeNPs reduced by ascorbic acid and stabilized by polyvinyl alcohol (PVA) or chitosan (CS) had no antibacterial action on *E. coli* (Boroumand et al., 2019).

Nanoparticle size is an essential factor that influences their antimicrobial potential. Small-sized SeNPs with low negative surface charge have antibacterial activity more than the larger and more negative ones (Zonaro et al., 2015; Huang et al., 2019). Also, smaller-sized nanoparticles such as ZnONPs (Raghupathi et al., 2011), AgNPs (Yamamoto, 2001), CuONPs (Azam et al., 2012), and AuNPs (Mihai and Malaisteanu, 2013) exhibit a stronger antimicrobial action compared to the larger one.

Nonbactericidal effect of the prepared SeNPs may be associated with their large size (34 to 125 nm) and the high negative charge on their surface (zeta potential -22.4 mV). The increase in nanoparticle size reduces their ability to penetrate cell membranes (Barua and Mitragotri, 2014). The bacterial cell membrane is negatively charged (Chung et al., 2004) that causes electrostatic repulsion with the more negatively charged nanoparticles (Hamouda and Baker Jr, 2000; Stoimenov et al., 2002; Huang et al., 2019).

### 3.2 Cytotoxicity of Biosynthesized SeNPs

Cytotoxicity is an essential assay that determines the safety of biosynthesized SeNPs to be used as a therapeutic drug. In addition, the toxicity of SeNPs is an essential factor that influences their bioavailability as low toxicity allows high bioavailability (Pandiyani et al., 2022). Cytotoxicity of SeNPs to mouse normal liver cells can be detected by an SRB assay. This colorimetric assay is based on measuring the absorbance of SRB dye binding to amino acids of cellular proteins that is related to the number of viable cells.

Cell viability percentage of mouse normal liver cells incubated with nine SeNPs concentrations (1,

3, 10, 30, 100, 150, 200, 250, and 300  $\mu\text{g}/\text{mL}$ ) were 102.66, 98.06, 94.24, 93.70, 90.06, 89.22, 88.14, 85.34, and 82.75 % respectively. In the SRB assay, the calculated  $\text{IC}_{50}$  value of *Saccharomyces cerevisiae*-derived SeNPs was above 300  $\mu\text{g}/\text{mL}$  (the highest concentration that is used) as shown in Figure 3. The present yeast-synthesized SeNPs had noncytotoxic action. Compared with other studies, the in vitro cytotoxicity of SeNPs synthesized by *Penicillium corylophilum* was tested against the normal cell lines with  $\text{IC}_{50}$  values of 171.8 and 104.3 ppm for Wi 38 and Caco-2 cell lines, respectively (Salem et al., 2021). Also, that of SeNPs synthesized by *Spirulina platensis* was 849.21 and 233.08  $\mu\text{g}/\text{mL}$  in normal cells of the liver and kidney, respectively (Abbas et al., 2021). It was found that 100  $\mu\text{g}/\text{mL}$  of SeNPs synthesized using yeast-fermented broth had a very little cytotoxic action against the normal cell line of the Chinese hamster ovary (Goud et al., 2016). Meanwhile, the cytotoxicity of different concentrations of SeNPs stabilized by aminated yeast glucan was tested. The concentrations ranging from 10 to 100  $\mu\text{g}/\text{mL}$  were noncytotoxic concentrations against RAW264.7 cells and 50  $\mu\text{g}/\text{mL}$  could stimulate cell proliferation (Sun et al., 2023).

Cytotoxicity of nanoparticles is dependent on both the synthesis method and the type of stabilizing biocompounds coating nanoparticles (Chen et al., 2008; Abbas et al., 2021). Also, it is affected by their size and shape (Woźniak et al., 2017). There is an inverse relation between the size of nanoparticles and their toxicity. The small-sized nanoparticles showed higher toxicity than the larger ones (Pan et al., 2007; Hanan et al., 2018). It was suggested that the aggregation of small-sized nanoparticles on the cell membrane causes cell death and increases the cytotoxicity action of nanoparticles (Jiang et al., 2010; Woźniak et al., 2017). In addition, the smaller nanoparticles can highly penetrate cells more easily than the larger ones (Barua and Mitragotri, 2014). Our results assumed that the noncytotoxic effect of the yeast-synthesized SeNPs could be attributed to their large size (34 to 125 nm), zeta potential (-22.4 mV), and PDI (0.503) that decrease their cellular penetration and aggregation on the cell membrane.

According to our research result, the used concentrations of biogenic SeNPs have no cytotoxic effect on mouse normal liver cells in a dose-dependent manner. Therefore, the yeast-mediated SeNPs can be used as a safe nontoxic antimicrobial, antiradical, and anti-inflammatory drug.

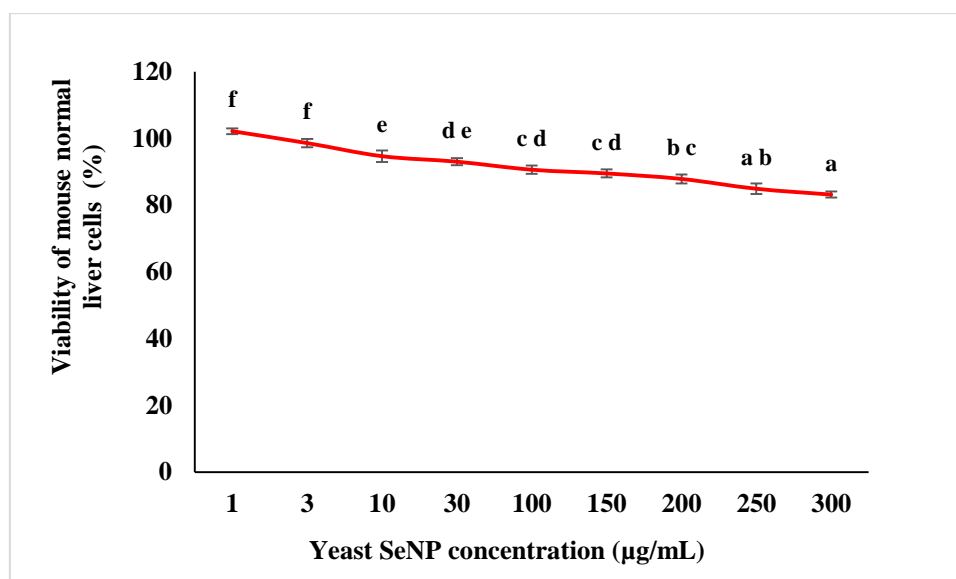


**Fig. 3. Cell viability of mouse normal liver cells at various concentrations of yeast-mediated SeNPs. Cell viability was measured using an SRB assay.**

Data represent the mean values of three experiments  $\pm$  SE. Values with similar superscript letters are insignificantly different while the different superscript letters are significantly different. The least significant difference (LSD) was 3.62 ( $p < 0.05$ ).

### 3.3 Antiradical Activity

A free radical is considered as one of the important factors that cause damage to tissue and organs. The presence of free radicals leads to an imbalance between free radical stress and antiradical protection activity in the living organism (Re et al., 1999). Nanoparticles are promising antiradical radical scavengers that have the ability to remove and scavenge excessive free radicals due to their small size (Faramarzi et al., 2020; Yang et al., 2023). Furthermore, selenoproteins are essential proteins containing the selenium element and naturally exhibit antiradical activity (Pappas et al., 2008).

Antiradical activity of yeast-mediated SeNPs can be detected by measuring their ability to scavenge the free radical compared to ascorbic acid as a standard agent. The test was done by using DPPH that is widely used to test antiradical activity. Both ascorbic acid and the prepared SeNPs reduced DPPH free radical converting DPPH color from violet (radical form) to pale yellow (reduced form). As shown in Figure 4, the antiradical activity of ascorbic acid and SeNPs was detected at 50, 100, 150, 200, and 250  $\mu\text{g/mL}$  against DPPH radical. Scavenging activities of ascorbic acid were 76.24, 85.61, 88.39, 91.35, and 92.55%, respectively and that of tested SeNPs were 54.24, 60.35, 63.26, 50.27, and 52.90%, respectively. The inhibitory concentration of SeNPs that is required for scavenging 50% of free radicals ( $\text{IC}_{50}$ ) was 45.87  $\mu\text{g/mL}$ . It is worthy to mention that nontoxic dose of 150  $\mu\text{g/mL}$  SeNPs showed the highest antiradical action (63.26%).

Other data obtained from the previous studies also indicate the capability of biogenic SeNPs to be one of the powerful oxidizing agents. The percentage of inhibition activity of *Saccharomyces cerevisiae*-synthesized SeNPs ranged from 20.8 to 48.5% based on the amount of selenium salt that was used (Faramarzi et al., 2020). The antiradical activity of 500  $\mu\text{g/mL}$  SeNPs synthesized by yeast-fermented broth was 79 % and the  $\text{IC}_{50}$  value was 236  $\mu\text{g/mL}$  (Goud et al., 2016).

Antioxidant activity of the yeast *Nematospora coryli*-derived SeNPs using the DPPH test was detected. Different SeNP concentrations had an antioxidant action that increased when the concentration increased (Rasouli, 2019). *Penicillium verhagenii*-mediated SeNPs showed  $19.3 \pm 4.5\%$  inhibition percentage at a concentration of  $1.95 \mu\text{g mL}^{-1}$  and  $86.8 \pm 0.6\%$  at a concentration of  $1000 \mu\text{g mL}^{-1}$  (Nassar et al., 2023). The concentration of 200  $\mu\text{g/mL}$  biosynthesized SeNPs by *Bacillus* sp. MSh-1 had an antiradical capacity percentage equal to  $23.1 \pm 3.4\%$  (Forootanfar et al., 2014).

The antiradical capacity of SeNPs may be attributed to their hydrogen transferring activity and surface charge, in addition to the presence of a yeast-formed capping material on the SeNPs' surface that contains hydroxyl (OH) function group that was detected by FTIR analysis (Zhang et al., 2019; Dumore and Mukhopadhyay, 2020). Small particle size and large surface area of SeNPs also improve the antiradical activity by providing a large number of reactive sites required for free radical elimination (Xiao et al., 2017; Tang et al., 2021; Chen et al., 2022; Yang et al., 2023). SeNPs can replace the



free radical present at the nitrogen atom of DPPH by hydrogen donation converting  $\text{DPPH}^{\bullet}$  (DPPH radical) to DPPH-H. The free radical scavenging mechanism of SeNPs is based on their hydrogen- or electron-donating capacity (Dumore and Mukhopadhyay, 2020).

Our results suggest that the prepared SeNPs using *Saccharomyces cerevisiae* can be used as an antiradical agent at nontoxic concentrations.

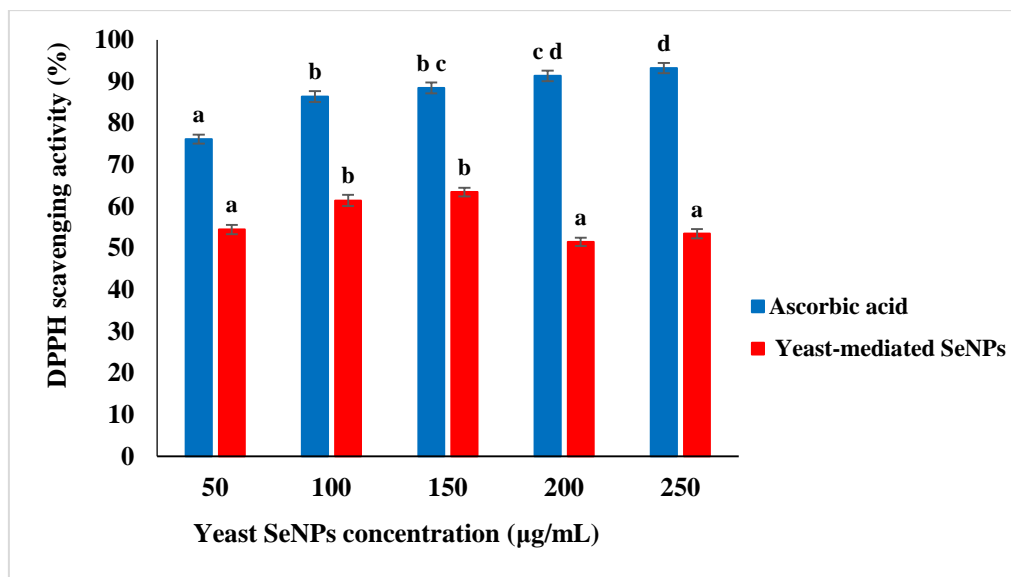


**Fig. 4. DPPH free radical scavenging activity of different concentrations of yeast-mediated SeNPs compared with ascorbic acid as a standard antiradical agent.**

Data represent the mean values of three experiments  $\pm$  SE. Values with similar superscript letters are insignificantly different while the different superscript letters are significantly different. The least significant difference (LSD) of ascorbic acid was 3.42 and that of SeNPs was 3.73 ( $p < 0.05$ ).

### 3.4 Anti-inflammatory Activity

An SRB assay was used to measure the cytotoxicity of SeNPs on macrophage cells. This measurement is essential to detect the nontoxic SeNP doses that would be used for anti-inflammatory tests of SeNPs. As shown in Figure 5a, cell viability percentages of RAW264.7 macrophage cells exposed to different SeNP concentrations (20, 30, 40, 50, and 100 µg/mL) were 102.34, 99.98, 99.68, 97.36, and 88.88%, respectively. The value of  $\text{IC}_{50}$  was above 100 µg/mL.

The anti-inflammatory activity of SeNPs was detected by measuring the concentration of NO produced by RAW264.7 macrophage cells as a response to LPS-induced inflammation. The inhibitory percentages of five SeNP concentrations (20, 30, 40, 50, and 100 µg/mL) were 12.05, 13.43, 23.24, 27.20, and 41.34%, respectively (Figure 5b). According to the used concentrations, the highest anti-inflammatory activity (41.34%) was shown at 100 µg/mL SeNPs which represents a nontoxic concentration. The results revealed that the different concentrations of prepared SeNPs (20–100 µg/mL) have no toxicity effect on RAW264.7 macrophage cells. As discussed previously, the

nontoxic effect of SeNPs may be attributed to their large size that affects their ability to penetrate a living cell and aggregate on its membrane.

Pretreatment with yeast-derived SeNPs inhibits the production of NO induced by LPS in RAW264.7 macrophage cells and therefore reduces its inflammatory effect. Our results agree with those obtained by Sun et al. (2023), where they tested the anti-inflammatory action of SeNPs stabilized by aminated yeast glucan. At several concentrations ranging from 10 to 100 µg/mL, the used nanoparticles showed an anti-inflammatory effect on RAW264.7 macrophage cells with a nontoxic effect. Meanwhile, the mycogenic SeNPs synthesized by the endophytic fungus *Curvularia* sp. LCJ413 showed an anti-inflammatory potential. At 50 µg/mL SeNPs, the inhibition activity for bovine serum albumin denaturation was  $80.55 \pm 2.7\%$  and that for egg albumin was  $76.01 \pm 3.1\%$  (Kathiravan et al., 2023). A recent study proved that SeNPs-enriched *Enterococcus durans* A8-1 as a probiotic bacterium possesses anti-inflammatory action (Liu et al., 2022).

Macrophages are essential leukocytes that attack irritants causing many infectious, immunological, and degenerative diseases (Liu et al., 2020; Mi et al., 2022). Nitric oxide has a critical role in the inflammation process where macrophage cells secrete NO as proinflammatory cytokines as a defense mechanism. Production of NO in a proper amount helps in body defense while excessive production causes body damage and various inflammatory diseases (Guzik et al., 2003; Guo et al., 2018; Mi et al., 2022). It was suggested that selenium has anti-inflammatory activity due to its action on signaling pathways of macrophages (Duntas, 2009; Javdani and Barzegar, 2023). Mi et

al. (2022) suggested that SeNPs can inhibit inflammation stimulated by LPS through downregulation of PI3K/Akt/NF- $\kappa$ B pathways. Other research recorded that SeNPs stabilized and capped by aminated yeast glucan could reduce the transcription of iNOS, subsequently inhibiting the production of NO in RAW 264.7 macrophage cells induced by LPS showing a good anti-inflammatory potential (Sun et al., 2023).

Our research revealed that yeast-biosynthesized SeNPs can be used as a nontoxic anti-inflammatory drug instead of other commercial drugs that have side effects on body health.

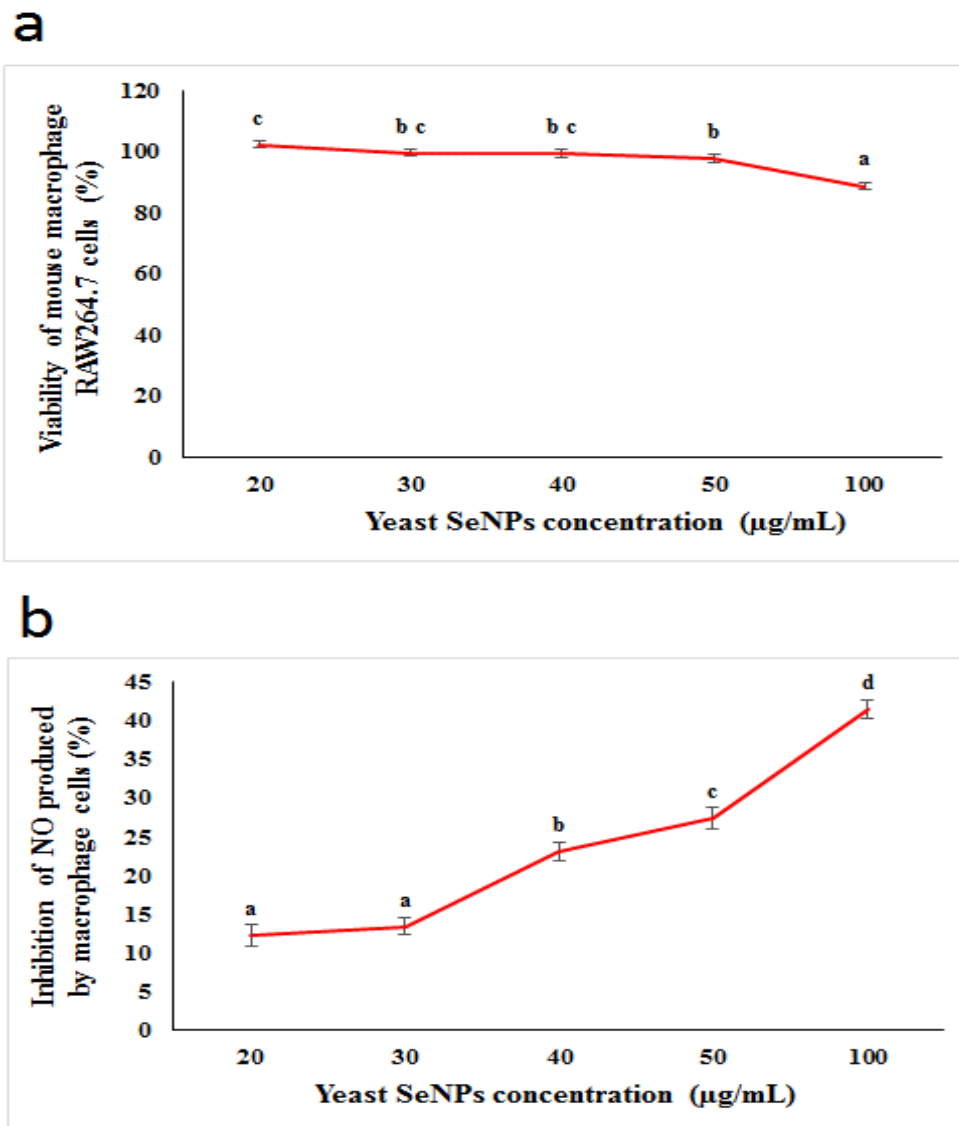


**Fig. 5.** (a) Cell viability of RAW 264.7 cells at various concentrations of yeast-mediated SeNPs. Cell viability was measured using an SRB assay. (b) Inhibitory effects of yeast-derived SeNPs on the production of nitric oxide. The least significant difference (LSD) at  $p < 0.05$  was 3.61 for cell viability and 3.8 for inhibition of nitric oxide.

Data represents the mean values of three experiments  $\pm$  SE. Values with similar superscript letters are insignificantly different while the different superscript letters are significantly different.

## Conclusion

This study suggested that SeNPs can be synthesized by using baker's yeast (*Saccharomyces cerevisiae*) as a biological and green method. Based on TEM results, SeNPs have a spherical shape and size ranging from 34 to 125 nm and the average size detected with DLS was 173.9 nm. As detected from peaks of functional groups present in FTIR spectrum, yeast-fabricated SeNPs were coated with proteins produced by yeast cells. In addition, negative charges (-22.4 mV) on SeNPs surface allow repulsion between particles. XRD showed that the prepared nanoparticles are naturally amorphous. Yeast-synthesized SeNPs exhibited a nontoxic effect on mouse normal liver and RAW264.7 macrophage cells according to an SRB assay. Moreover, they showed antiradical action against DPPH free radical and anti-inflammatory capacity against NO secretion by macrophage cells. So, we can conclude that SeNPs synthesized by yeast can be used as a drug for the treatment of both free radical stress and inflammation at noncytotoxic doses up to 300 µg/mL. As far as the authors are aware, this is the first research that detects the cytotoxicity and anti-inflammatory effect of *Saccharomyces cerevisiae*-mediated SeNPs.

## References

- Abbas, H. S., Abou Baker, D. H., Ahmed, E. A. (2021) Cytotoxicity and antimicrobial efficiency of selenium nanoparticles biosynthesized by *Spirulina platensis*. *Archives of Microbiology*, **203**(2), 523-532.
- Abd El-Ghany, M. N., Hamdi, S. A., Korany, S. M., Elbaz, R. M., Emam, A. N., Farahat, M. G. (2023) Biogenic silver nanoparticles produced by soil rare actinomycetes and their significant effect on *Aspergillus*-derived mycotoxins. *Microorganisms*, **11**(4), 1006.
- Abegunde, O. O., Akinlabi, E. T., Oladijo, O. P., Akinlabi, S., Ude, A. U. (2019) Overview of thin film deposition techniques. *AIMS Materials Science*, **6** (2), 174-199.
- Ahmed, A. H. H., Mohamed, M. F. A., Allam, R. M., Nafady, A., Mohamed, S. K., Gouda, A. E., Beshr, E. A. M. (2022) Design, synthesis, and molecular docking of novel pyrazole-chalcone analogs of lonazolac as 5-LOX, iNOS and tubulin polymerization inhibitors with potential anticancer and anti-inflammatory activities. *Bioorg Chem*, **129**, 106171.
- Akçay, F. A., Avcı, A. (2020) Effects of process conditions and yeast extract on the synthesis of selenium nanoparticles by a novel indigenous isolate *Bacillus* sp. EKT1 and characterization of nanoparticles. *Archives of Microbiology*, **202**(8), 2233-2243.
- Allam, R. M., Al-Abd, A. M., Khedr, A., Sharaf, O. A., Nofal, S. M., Khalifa, A. E., Mosli, H. A., Abdel-Naim, A. B. (2018) Fingolimod interrupts the cross talk between estrogen metabolism and sphingolipid metabolism within prostate cancer cells. *Toxicology Letters*, **291**, 77-85.
- Alsammaraie, F. K., Wang, W., Zhou, P., Mustapha, A., Lin, M. (2018) Green synthesis of silver nanoparticles using turmeric extracts and investigation of their antibacterial activities. *Colloids and surfaces B: Biointerfaces*, **171**, 398-405.
- Anandalakshmi, K., Venugobal, J., Ramasamy, V. (2016) Characterization of silver nanoparticles by green synthesis method using *Petalium murex* leaf extract and their antibacterial activity. *Applied nanoscience*, **6**, 399-408
- Ansari, A. Q., Ahmed, S. A., Waheed, M., Juned, S. (2013) Extraction and determination of antioxidant activity of *Withania somnifera* Dunal. *Eur J Exp Biol*, **3** (5), 502-507.
- Arokiyaraj, S., Dinesh Kumar, V., Elakya, V., Kamala, T., Park, S. K., Ragam, M., Saravanan, M., Bououdina, M., Valan Arasu, M., Kovendan, K., Vincent S., (2015) Biosynthesized silver nanoparticles using floral extract of *Chrysanthemum indicum* L.—potential for malaria vector control. *Environmental Science and Pollution Research*, **22**, 9759-9765.
- Attia, Y. A., Farag, Y. E., Mohamed, Y. M., Hussien, A. T., Youssef, T. (2016) Photo-extracellular synthesis of gold nanoparticles using Baker's yeast and their anticancer evaluation against Ehrlich ascites carcinoma cells. *New Journal of Chemistry*, **40**(11), 9395-9402.
- Azam, A., Ahmed, A. S., Oves, M., Khan, M. S., Memic, A. (2012) Size-dependent antimicrobial properties of CuO nanoparticles against Gram-positive and-negative bacterial strains. *Int J Nanomedicine*, 3527-3535.
- Bai, K., Hong, B., Tan, R., He, J., Hong, Z. (2020) Selenium nanoparticles-embedded chitosan microspheres and their effects upon alcohol-induced gastric mucosal injury in rats: Rapid preparation, oral delivery, and gastroprotective potential of selenium nanoparticles. *International journal of nanomedicine*, 1187-1203.
- Bartosiak, M., Giersz, J., Jankowski, K. (2019) Analytical monitoring of selenium nanoparticles green synthesis using photochemical vapor generation coupled with MIP-OES and UV-Vis spectrophotometry. *Microchemical Journal*, **145**, 1169-1175.
- Barua, S., Mitraborti, S. (2014) Challenges associated with penetration of nanoparticles across cell and tissue barriers: a review of current status and future prospects. *Nano today*, **9**(2), 223-243.
- Boroumand, S., Safari, M., Shaabani, E., Shirzad, M., Faridi-Majidi, R. (2019) Selenium nanoparticles: Synthesis, characterization and study of their cytotoxicity, antioxidant and antibacterial activity. *Materials Research Express*, **6**.
- Carrapiço, A., Martins, M. R., Caldeira, A. T., Mirão, J., Dias, L. (2023) Biosynthesis of metal and metal oxide nanoparticles using microbial cultures:

- Mechanisms, antimicrobial activity and applications to cultural heritage. *Microorganisms*, **11**(2), 378.
- Chen, T., Wong, Y.-S., Zheng, W., Bai, Y., Huang, L. (2008) Selenium nanoparticles fabricated in *Undaria pinnatifida* polysaccharide solutions induce mitochondria-mediated apoptosis in A375 human melanoma cells. *Colloids and surfaces B: Biointerfaces*, **67**(1), 26-31.
- Chen, Y., Stoll, S., Sun, H., Liu, X., Liu, W., Leng, X. (2022) Stability and surface properties of selenium nanoparticles coated with chitosan and sodium carboxymethyl cellulose. *Carbohydrate polymers*, **278**, 118859.
- Chung, Y.-C., Su, Y. P., Chen, C.-C., Jia, G., Wang, H. L., Wu, J. G., Lin, J. G. (2004) Relationship between antibacterial activity of chitosan and surface characteristics of cell wall. *Acta pharmacologica sinica*, **25**(7), 932-936.
- Dang, H., Meng, M. H. W., Zhao, H., Iqbal, J., Dai, R., Deng, Y., Lv, F. (2014) Luteolin-loaded solid lipid nanoparticles synthesis, characterization, & improvement of bioavailability, pharmacokinetics in vitro and vivo studies. *Journal of Nanoparticle Research*, **16**, 1-10.
- Devi, H. S., Boda, M. A., Shah, M. A., Parveen, S., Wani, A. H. (2019) Green synthesis of iron oxide nanoparticles using *Platanus orientalis* leaf extract for antifungal activity. *Green Processing and Synthesis*, **8**(1), 38-45.
- Dinc, S. K., Vural, O. A., Kayhan, F. E., San Keskin, N. O. (2022) Facile biogenic selenium nanoparticle synthesis, characterization and effects on oxidative stress generated by UV in microalgae. *Particuology*, **70**, 30-42.
- Dubadi, R., Huang, S. D., Jaroniec, M. (2023) Mechanochemical synthesis of nanoparticles for potential antimicrobial applications. *Materials*, **16**(4), 1460.
- Dumore, N. S., Mukhopadhyay, M. (2020) Antioxidant properties of aqueous selenium nanoparticles (ASeNPs) and its catalysts activity for 1, 1-diphenyl-2-picrylhydrazyl (DPPH) reduction. *Journal of Molecular Structure*, **1205**, 127637.
- Duntas, L. H. (2009) Selenium and inflammation: underlying anti-inflammatory mechanisms. *Horm Metab Res*, **41**(6), 443-447.
- El-Khawaga, A. M., Elsayed, M. A., Gobara, M., Suliman, A. A., Hashem, A. H., Zäher, A. A., Mohsen, M., Salem, S. S. (2023) Green synthesized ZnO nanoparticles by *Saccharomyces cerevisiae* and their antibacterial activity and photocatalytic degradation. *Biomass Conversion and Biorefinery*, 1-12.
- Faramarzi, S., Anzabi, Y., Jafarizadeh-Malmiri, H. (2020) Nanobiotechnology approach in intracellular selenium nanoparticle synthesis using *Saccharomyces cerevisiae*—fabrication and characterization. *Archives of Microbiology*, **202**(5), 1203-1209.
- Fardsadegh, B., Jafarizadeh-Malmiri, H. (2019) Aloe vera leaf extract mediated green synthesis of selenium nanoparticles and assessment of their in vitro antimicrobial activity against spoilage fungi and pathogenic bacteria strains. *Green Processing and Synthesis*, **8**(1), 399-407.
- Fardsadegh, B., Vaghari, H., Mohammad-Jafari, R., Najian, Y., Jafarizadeh-Malmiri, H. (2019) Biosynthesis, characterization and antimicrobial activities assessment of fabricated selenium nanoparticles using *Pelargonium zonale* leaf extract. *Green Processing and Synthesis*, **8**(1), 191-198.
- Forootanfar, H., Adeli-Sardou, M., Nikkhoo, M., Mehrabani, M., Amir-Heidari, B., Shahverdi, A. R., Shakibaie, M. (2014) Antioxidant and cytotoxic effect of biologically synthesized selenium nanoparticles in comparison to selenium dioxide. *Journal of Trace Elements in Medicine and Biology*, **28**(1), 75-79.
- Francis, T., Rajeshkumar, S., Roy, A., Lakshmi, T. (2020) Anti-inflammatory and cytotoxic effect of arrow root mediated selenium nanoparticles. *Pharmacognosy Journal*, **12**(6).
- Goud, K. G., Veldurthi, N. K., Vithal, M., Reddy, G. (2016) Characterization and evaluation of biological and photocatalytic activities of selenium nanoparticles synthesized using yeast fermented broth. *Journal of Materials NanoScience*, **3**(2), 33-40.
- Guo, M., Xiao, J., Sheng, X., Zhang, X., Tie, Y., Wang, L., Zhao, L., Ji, X. (2018) Ginsenoside Rg3 mitigates atherosclerosis progression in diabetic apoE<sup>-/-</sup> mice by skewing macrophages to the M2 phenotype. *Front Pharmacol*, **9**, 464.
- Guzik, T. J., Korbout, R., Adamek-Guzik, T. (2003) Nitric oxide and superoxide in inflammation and immune regulation. *J Physiol Pharmacol*, **54**(4), 469-487.
- Hamouda, T., Baker Jr, J. (2000) Antimicrobial mechanism of action of surfactant lipid preparations in enteric Gram-negative bacilli. *Journal of applied microbiology*, **89**(3), 397-403.
- Hanan, N. A., Chiu, H. I., Ramachandran, M. R., Tung, W. H., Mohamad Zain, N. N., Yahaya, N., Lim, V. (2018) Cytotoxicity of plant-mediated synthesis of metallic nanoparticles: a systematic review. *Int J Mol Sci*, **19**(6), 1725.
- Hashem, A. H., Khalil, A. M. A., Reyad, A. M., Salem, S. S. (2021) Biomedical applications of mycosynthesized selenium nanoparticles using *Penicillium expansum* ATTC 36200. *Biological Trace Element Research*, 1-11.
- Huang, J., Li, Q., Sun, D., Lu, Y., Su, Y., Yang, X., Wang, H., Wang, Y., Shao, W., He, N. (2007) Biosynthesis of silver and gold nanoparticles by novel sundried *Cinnamomum camphora* leaf. *Nanotechnology*, **18**(10), 105104.
- Huang, T., Holden, J. A., Heath, D. E., O'Brien-Simpson, N. M., O'Connor, A. J. (2019) Engineering highly effective antimicrobial selenium nanoparticles through control of particle size. *Nanoscale*, **11**(31), 14937-14951.
- Hulkoti, N. I., Taranath, T. (2014) Biosynthesis of nanoparticles using microbes—a review. *Colloids and surfaces B: Biointerfaces*, **121**, 474-483.

- Hussain, M., Ceccarelli, R., Marchisio, D., Fino, D., Russo, N., Geobaldo, F. (2010) Synthesis, characterization, and photocatalytic application of novel TiO<sub>2</sub> nanoparticles. *Chemical Engineering Journal*, **157**(1), 45-51.
- Jalalian, S. H., Ramezani, M., Abnous, K., Taghdisi, S. M. (2018) Targeted co-delivery of epirubicin and NAS-24 aptamer to cancer cells using selenium nanoparticles for enhancing tumor response *in vitro* and *in vivo*. *Cancer Lett*, **416**, 87-93.
- Javdani, M., Barzegar, A. (2023) Application of chitosan hydrogels in traumatic spinal cord injury; a therapeutic approach based on the anti-inflammatory and antioxidant properties of selenium nanoparticles. *Frontiers in Biomedical Technologies*.
- Jia, H., Huang, S., Cheng, S., Zhang, X., Chen, X., Zhang, Y., Wang, J., Wu, L. (2022) Novel mechanisms of selenite reduction in *Bacillus subtilis* 168: Confirmation of multiple-pathway mediated remediation based on transcriptome analysis. *Journal of Hazardous Materials*, **433**, 128834.
- Jiang, X., Weise, S., Hafner, M., Röcker, C., Zhang, F., Parak, W. J., Nienhaus, G. U. (2010) Quantitative analysis of the protein corona on FePt nanoparticles formed by transferrin binding. *Journal of The Royal Society Interface*, **7**(suppl\_1), S5-S13.
- Karthik, K., Cheriyan, B. V., Rajeshkumar, S., Gopalakrishnan, M. (2024) A review on selenium nanoparticles and their biomedical applications. *Biomedical Technology*, **6**, 61-74.
- Kathiravan, A., Udayan, E., Rajeshkumar, S., Gnanadoss, J. J. (2023) Unveiling the Biological Potential of Mycosynthesized Selenium Nanoparticles from Endophytic Fungus *Curvularia* sp. LCJ413. *BioNanoScience*, 1-20.
- Khalil, N. M., Abd El-Ghany, M. N., Rodríguez-Couto, S. (2019) Antifungal and anti-mycotoxin efficacy of biogenic silver nanoparticles produced by *Fusarium chlamydosporum* and *Penicillium chrysogenum* at non-cytotoxic doses. *Chemosphere*, **218**, 477-486.
- Khan, I., Saeed, K., Khan, I. (2019) Nanoparticles: Properties, applications and toxicities. *Arabian journal of chemistry*, **12**(7), 908-931.
- Kharchenko, Y., Lastovetska, L., Maslak, V., Sidorenko, M., Vasylenko, V., Shydlovska, O. (2022) Antibacterial Activity of Green Synthesised Silver Nanoparticles on *Saccharomyces cerevisiae*. *Applied Sciences*, **12**(7), 3466.
- Khurana, A., Tekula, S., Saifi, M. A., Venkatesh, P., Godugu, C. (2019) Therapeutic applications of selenium nanoparticles. *Biomedicine & Pharmacotherapy*, **111**, 802-812.
- Kim, C., Le, D., Lee, M. (2021) Diterpenoids Isolated from *Podocarpus macrophyllus* Inhibited the Inflammatory Mediators in LPS-Induced HT-29 and RAW 264.7 Cells. *Molecules*, **26**(14), 4326.
- Kora, A. J. (2018a) *Bacillus cereus*, selenite-reducing bacterium from contaminated lake of an industrial area: a renewable nanofactory for the synthesis of selenium nanoparticles. *Bioresources and Bioprocessing*, **5** (1), 30.
- Kora, A. J. (2018b) Tree gum stabilised selenium nanoparticles: characterisation and antioxidant activity. *IET Nanobiotechnology*, **12**(5), 658-662.
- Korbekandi, H., Mohseni, S., Mardani Jouneghani, R., Pourhossein, M., Iravani, S. (2016) Biosynthesis of silver nanoparticles using *Saccharomyces cerevisiae*. *Artif Cells Nanomed Biotechnol*, **44**(1), 235-239.
- Li, X., Xu, H., Chen, Z.-S., Chen, G. (2011) Biosynthesis of nanoparticles by microorganisms and their applications. *Journal of nanomaterials*, **2011**, 1-16.
- Lian, S., Diko, C. S., Yan, Y., Li, Z., Zhang, H., Ma, Q., Qu, Y. (2019) Characterization of biogenic selenium nanoparticles derived from cell-free extracts of a novel yeast *Magnusiomyces ingens*. *3 Biotech*, **9**, 1-8.
- Liu, J., Shi, L., Tuo, X., Ma, X., Hou, X., Jiang, S., Lv, J., Cheng, Y., Guo, D., Han, B. (2022) Preparation, characteristic and anti-inflammatory effect of selenium nanoparticle-enriched probiotic strain *Enterococcus durans* A8-1. *Journal of Trace Elements in Medicine and Biology*, **74**, 127056.
- Liu, Y., Perumalsamy, H., Kang, C. H., Kim, S. H., Hwang, J. S., Koh, S. C., Yi, T. H., Kim, Y. J. (2020) Intracellular synthesis of gold nanoparticles by *Glucacetobacter liquefaciens* for delivery of peptide CopA3 and ginsenoside and anti-inflammatory effect on lipopolysaccharide-activated macrophages. *Artif Cells Nanomed Biotechnol*, **48** (1), 777-788. doi:10.1080/21691401.2020.1748639
- Martínez-Esquivias, F., Gutiérrez-Angulo, M., Pérez-Larios, A., Sánchez-Burgos, J. A., Becerra-Ruiz, J. S., Guzmán-Flores, J. M. (2022) Anticancer activity of selenium nanoparticles *in vitro* studies. *Anti-Cancer Agents in Medicinal Chemistry (Formerly Current Medicinal Chemistry-Anti-Cancer Agents)*, **22**(9), 1658-1673.
- McNamara, K., Tofail, S. A. (2017) Nanoparticles in biomedical applications. *Advances in Physics: X*, **2**(1), 54-88.
- Mi, X.-j., Le, H.-M., Lee, S., Park, H.-R., Kim, Y.-J. (2022) Silymarin-functionalized selenium nanoparticles prevent LPS-induced inflammatory response in RAW264.7 cells through downregulation of the PI3K/Akt/NF- $\kappa$ B pathway. *ACS omega*, **7**(47), 42723-42732.
- Mihai, S., Malaisteanu, M. (2013) Size-dependent antibacterial of gold colloids. *Revista de Chimie-Bucharest*, **64**, 105-107.
- Miroliaee, A. E., Esmaily, H., Vaziri-Bami, A., Baeri, M., Shahverdi, A. R., Abdollahi, M. (2011) Amelioration of experimental colitis by a novel nanoselenium-silymarin mixture. *Toxicology mechanisms and methods*, **21** (3), 200-208.
- Mohammad, R. (2019) Biosynthesis of Selenium Nanoparticles Using Yeast *Nematospira Coryli* and Examination of Their Anti-Candida and Anti-Oxidant Activities. *IET nanobiotechnology*, **13** (2), 214-18.
- Motazedi, R., Rahaiee, S., Zare, M. (2020) Efficient biogenesis of ZnO nanoparticles using extracellular

- extract of *Saccharomyces cerevisiae*: Evaluation of photocatalytic, cytotoxic and other biological activities. *Bioorganic chemistry*, **101**, 103998.
- Mudshinge, S. R., Deore, A. B., Patil, S., Bhalgat, C. M. (2011) Nanoparticles: Emerging carriers for drug delivery. *Saudi pharmaceutical journal*, **19** (3), 129-141.
- Nassar, A.-R. A., Eid, A. M., Atta, H. M., El Naghy, W. S., Fouda, A. (2023) Exploring the antimicrobial, antioxidant, anticancer, biocompatibility, and larvicidal activities of selenium nanoparticles fabricated by endophytic fungal strain *Penicillium verhagenii*. *Scientific reports*, **13** (1), 9054.
- Nowack, B., Bucheli, T. D. (2007) Occurrence, behavior and effects of nanoparticles in the environment. *Environmental pollution*, **150** (1), 5-22.
- Pan, Y., Neuss, S., Leifert, A., Fischler, M., Wen, F., Simon, U., Schmid, G., Brandau, W., Jahn-Dechent, W. (2007) Size-dependent cytotoxicity of gold nanoparticles. *Small*, **3** (11), 1941-1949.
- Pandiyan, I., Sri, S. D., Indiran, M. A., Rathinavelu, P. K., Prabakar, J., Rajeshkumar, S. (2022) Antioxidant, anti-inflammatory activity of *Thymus vulgaris*-mediated selenium nanoparticles: An *in vitro* study. *Journal of Conservative Dentistry: JCD*, **25** (3), 241.
- Pappas, A., Zoidis, E., Surai, P., Zervas, G. (2008) Selenoproteins and maternal nutrition. *Comparative Biochemistry and Physiology Part B: Biochemistry and Molecular Biology*, **151**(4), 361-372.
- Pilotto, A., Sancarolo, D., Addante, F., Scarcelli, C., Franceschi, M. (2010) Non-steroidal anti-inflammatory drug use in the elderly. *Surgical oncology*, **19** (3), 167-172.
- Raghupathi, K. R., Koodali, R. T., Manna, A. C. (2011) Size-dependent bacterial growth inhibition and mechanism of antibacterial activity of zinc oxide nanoparticles. *Langmuir*, **27** (7), 4020-4028.
- Rasouli, M. (2019) *Biosynthesis of selenium nanoparticles using yeast Nematospira coryli and examination of their anti-candida and anti-oxidant activities*. *IET nanobiotechnology*, **13** (2): p. 214-218.
- Re, R., Pellegrini, N., Proteggente, A., Pannala, A., Yang, M., Rice-Evans, C. (1999) Antioxidant activity applying an improved ABTS radical cation decolorization assay. *Free radical biology and medicine*, **26** (9-10), 1231-1237.
- Salem, S. S. (2022) Bio-fabrication of selenium nanoparticles using Baker's yeast extract and its antimicrobial efficacy on food borne pathogens. *Applied Biochemistry and Biotechnology*, **194** (5), 1898-1910.
- Salem, S. S., Fouda, M. M., Fouda, A., Awad, M. A., Al-Olayan, E. M., Allam, A. A., Shaheen, T. I. (2021) Antibacterial, cytotoxicity and larvicidal activity of green synthesized selenium nanoparticles using *Penicillium corylophilum*. *Journal of Cluster Science*, **32**, 351-361.
- Saratale, R. G., Saratale, G. D., Shin, H. S., Jacob, J. M., Pugazhendhi, A., Bhaisare, M., Kumar, G. (2018) New insights on the green synthesis of metallic nanoparticles using plant and waste biomaterials: current knowledge, their agricultural and environmental applications. *Environmental Science and Pollution Research*, **25**, 10164-10183.
- Sarkar, J., Dey, P., Saha, S., Acharya, K. (2011) Mycosynthesis of selenium nanoparticles. *Micro & nano letters*, **6** (8), 599-602.
- Sasidharan, S., Balakrishnaraja, R. (2014) Comparison studies on the synthesis of selenium nanoparticles by various microorganisms. *Int. J. Pure Appl. Biosci*, **2**, 112-117.
- Shoebi, S., Mashreghi, M. (2017) Biosynthesis of selenium nanoparticles using *Enterococcus faecalis* and evaluation of their antibacterial activities. *Journal of Trace Elements in Medicine and Biology*, **39**, 135-139.
- Skehan, P., Storeng, R., Scudiero, D., Monks, A., McMahon, J., Vistica, D., Warren, J. T., Bokesch, H., Kenney, S., Boyd, M. R. (1990) New colorimetric cytotoxicity assay for anticancer-drug screening. *JNCI: Journal of the National Cancer Institute*, **82** (13), 1107-1112.
- Srivastava, N., Mukhopadhyay, M. (2013) Biosynthesis and structural characterization of selenium nanoparticles mediated by *Zooglea ramigera*. *Powder technology*, **244**, 26-29.
- Stoimenov, P. K., Klinger, R. L., Marchin, G. L., Klabunde, K. J. (2002) Metal oxide nanoparticles as bactericidal agents. *Langmuir*, **18**(17), 6679-6686.
- Sun, Y., Liang, L., Yi, Y., Meng, Y., Peng, K., Jiang, X., Wang, H. (2023) Synthesis, characterization and anti-inflammatory activity of selenium nanoparticles stabilized by aminated yeast glucan. *Int J Biol Macromol*, **125187**.
- Tang, L., Luo, X., Wang, M., Wang, Z., Guo, J., Kong, F., Bi, Y. (2021) Synthesis, characterization, *in vitro* antioxidant and hypoglycemic activities of selenium nanoparticles decorated with polysaccharides of *Gracilaria lemaneiformis*. *International journal of biological macromolecules*, **193**, 923-932.
- Tugarova, A. V., Mamchenkova, P. V., Dyatlova, Y. A., Kamnev, A. A. (2018) FTIR and Raman spectroscopic studies of selenium nanoparticles synthesised by the bacterium *Azospirillum thioophilum*. *Spectrochimica Acta Part A: Molecular and Biomolecular Spectroscopy*, **192**, 458-463.
- Visha, P., Nanjappan, K., Selvaraj, P., Jayachandran, S., Elango, A., Kumaresan, G. (2015) Biosynthesis and structural characteristics of selenium nanoparticles using *Lactobacillus acidophilus* bacteria by wet sterilization process. *International Journal of Advanced Veterinary Science and Technology*, **4**(1), 178-183.
- Woźniak, A., Malankowska, A., Nowaczyk, G., Grześkowiak, B. F., Tuśnio, K., Słomski, R., Zaleska-Medynska, A., Jurga, S. (2017) Size and shape-dependent cytotoxicity profile of gold nanoparticles for biomedical applications. *Journal of Materials Science: Materials in Medicine*, **28**, 1-11.

- Wu, Z., Ren, Y., Liang, Y., Huang, L., Yang, Y., Zafar, A., Hasan, M., Yang, F., Shu, X. (2021) Synthesis, characterization, immune regulation, and antioxidative assessment of yeast-derived selenium nanoparticles in cyclophosphamide-induced rats. *ACS omega*, **6**(38), 24585-24594.
- Xiao, Y., Huang, Q., Zheng, Z., Guan, H., Liu, S. (2017). Construction of a *Cordyceps sinensis* exopolysaccharide-conjugated selenium nanoparticles and enhancement of their antioxidant activities. *International journal of biological macromolecules*, **99**, 483-491.
- Xu, C., Qiao, L., Ma, L., Yan, S., Guo, Y., Dou, X., Zhang, B., Roman, A. (2019) Biosynthesis of polysaccharides-capped selenium nanoparticles using *Lactococcus lactis* NZ9000 and their antioxidant and anti-inflammatory activities. *Frontiers in microbiology*, **10**, 1632.
- Yamamoto, O. (2001) Influence of particle size on the antibacterial activity of zinc oxide. *International Journal of Inorganic Materials*, **3** (7), 643-646.
- Yang, Z., Hu, Y., Yue, P., Li, H., Wu, Y., Hao, X., Peng, F. (2023) Structure, stability, antioxidant activity, and controlled-release of selenium nanoparticles decorated with lichenan from *Usnea longissima*. *Carbohydrate polymers*, **299**, 120219.
- Ying, S., Guan, Z., Ofoegbu, P. C., Clubb, P., Rico, C., He, F., Hong, J. (2022) Green synthesis of nanoparticles: Current developments and limitations. *Environmental Technology & Innovation*, **26**, 102336.
- Zhang, S., Liu, Y., Gu, P., Ma, R., Wen, T., Zhao, G., Li, L., Ai, Y., Hu, C., Wang, X. (2019) Enhanced photodegradation of toxic organic pollutants using dual-oxygen-doped porous g-C<sub>3</sub>N<sub>4</sub>: Mechanism exploration from both experimental and DFT studies. *Applied Catalysis B: Environmental*, **248**, 1-10.
- Zhang, S., Song, S., Gu, P., Ma, R., Wei, D., Zhao, G., Wen, T., Jehan, T., Hu, B., Wang, X. (2019) Visible-light-driven activation of persulfate over cyano and hydroxyl group co-modified mesoporous gC<sub>3</sub>N<sub>4</sub> for boosting bisphenol A degradation. *Journal of Materials Chemistry A*, **7**(10), 5552-5560.
- Zonaro, E., Lampis, S., Turner, R. J., Qazi, S. J. S., Vallini, G. (2015) Biogenic selenium and tellurium nanoparticles synthesized by environmental microbial isolates efficaciously inhibit bacterial planktonic cultures and biofilms. *Front Microbiol*, **6**, 584.